Inorg. Chem. **2007**, *46*, 6775–6784

Silver Aggregation Caused by Stanna-*closo*-dodecaborate Coordination: Syntheses, Solid-State Structures and Theoretical Studies

Siegbert Hagen,[†] Hartmut Schubert,[†] Cäcilia Maichle-Mössmer,[†] Ingo Pantenburg,[‡] Florian Weigend,*[,#] and Lars Wesemann*[,†]

Institut für Anorganische Chemie, Universität Tübingen, Auf der Morgenstelle 18, 72076 Tübingen, Germany, Institut für Nanotechnologie, Forschungszentrum Karlsruhe, Postfach 3640, 76021 Karlsruhe, Germany, and Institut für Anorganische Chemie, Universität zu Köln, Greinstrasse 6, 50939 Köln, Germany

Received March 9, 2007

Stanna-*closo*-dodecaborate $[SnB_{11}H_{11}]^{2-}$ reacts as a nucleophile with various silver electrophiles ($[Ag(PMe_3)]^+$, $[Ag(PEt_3)]^+$, $[Ag(PPh_3)]^+$, and Ag^+) to form silver–tin bonds. Aggregation of two, three, or four units of $[\{Ag(SnB_{11}H_{11})(PR_3)\}_n]^{n-}$ (PPh_3, $n = 2$; PEt_3, $n = 3$; PMe_3, $n = 4$) was found, depending on the size of the coordinating phosphine. The structures of the silver–tin clusters in the solid state were determined by single-crystal X-ray diffraction. In these phosphine silver coordination compounds, the tin ligand exhibits μ_2- and μ_3-coordination with the silver atoms. From the reaction with silver nitrate, an octaanionic stanna-*closo*-dodecaborate coordination compound, $[Et_4N]_8[Ag_4(SnB_{11}H_{11})_6]$, was isolated. In this cluster, arranged as butterfly, the stannaborate shows various coordination modes at four silver atoms. In the reported silver–tin complexes, the silver–silver interatomic distances are in a range of 2.6326(10)–3.1424(6) Å. Silver–tin distances were found between 2.6416(5) and 3.1460(6) Å. Analysis of the molecular orbitals calculated by means of density functional theory shows that the LUMO of the core compound without $[SnB_{11}H_{11}]^{2-}$ units is always a totally symmetric combination of (mainly) s-orbitals of Ag atoms. This core is filled with electrons of the HOMOs of the $[SnB_{11}H_{11}]^{2-}$ units and is leading, in this way, to a stable compound.

Introduction

Controlled aggregation of the coinage metals is currently a field of active research. The factors influencing the stereochemistry and topology of these clusters are still of considerable interest and especially the development of synthetic procedures for the formation of large clusters plays an important role in the area of supramolecular chemistry and nanometer-sized clusters.[1,2] Furthermore, in the Cu, Ag, Au group, studies on metal−metal interactions with respect to relativistic effects have received a lot of attention over the last 30 years.[3−16] Interactions between silver atoms were systematically constructed by the reaction of heterocyclic carbene ligands with silver oxide.[17−18] Short metal−metal separations in a range of 2.7−2.9 Å were found in the solid-state structures of these trinuclear or tetranuclear silver−carbene clusters. From the reaction of [MesMgBr] with silver

* To whom correspondence should be addressed. E-mail: lars.wesemann@uni-tuebingen.de (L.W.); florian.weigend@int.fzk.de (F.W.).
† Universität Tübingen
# Forschungszentrum Karlsruhe.
‡ Universität zu Köln.

(1) *Metal Clusters in Chemistry*; Braunstein, P., Oro, L. A., Raithby, P. R., Eds.; Wiley-VCH: Weinheim, Germany, 1999.
(2) *Gold*; Schmidbaur, H., Ed.; Wiley: Chichester, U.K., 1999.
(3) Pyykkö, P. *Chem. Rev.* **1988**, *88*, 563.
(4) Pyykkö, P. *Chem. Rev.* **1997**, *97*, 597.
(5) Pyykkö, P.; Mendizabal, F. *Chem.—Eur. J.* **1997**, *3*, 1458.
(6) Schmidbaur, H. *Chem. Soc. Rev.* **1995**, 391.
(7) Fernandez, E. J.; Laguna, A.; Lopez-de-Luzuriaga, J. M.; Monge, M.; Pyykkö, P.; Runeberg, N. *Eur. J. Inorg. Chem.* **2002**, 750.
(8) Schwerdtfeger, P.; Boyd, P. D. W.; Burrell, A. K.; Robinson, W. T. *Inorg. Chem.* **1990**, *29*, 3593.
(9) Cotton, F. A.; Feng, X.; Matusz, M.; Poli, R. *J. Am. Chem. Soc.* **1988**, *110*, 7077.
(10) Schwerdtfeger, P.; Dolg, M.; Schwarz, W. H. E.; Bowmaker, G. A.; Boyd, P. D. W. *J. Chem. Phys.* **1989**, *91*, 1762.
(11) Jansen, M. *Angew. Chem.* **1987**, *26*, 1098.
(12) Jiang, Y.; Alvarez, S.; Hoffmann, R. *Inorg. Chem.* **1985**, *24*, 749.
(13) Pyykkö, P.; Zhao, Y. *Angew. Chem.* **1991**, *30*, 604.
(14) Schwerdtfeger, P.; Boyd, P. W. D. *Inorg. Chem.* **1992**, *31*, 327.
(15) Bowmaker, G. A.; Schmidbaur, H.; Krüger, S.; Rösch, N. *Inorg. Chem.* **1997**, *36*, 1754.
(16) Schwerdtfeger, P.; Hermann, H. L.; Schmidbaur, H. *Inorg. Chem.* **2003**, *42*, 1334.
(17) Catalano, V. J.; Malwitz, M. A. *Inorg. Chem.* **2003**, *42*, 5483.
(18) Garrison, J. C.; Simons, R. S.; Tessier, C. A.; Youngs, W. J. *J. Organomet. Chem.* **2003**, *673*, 1.

10.1021/ic700464d CCC: $37.00
Published on Web 06/30/2007

chloride, a polynuclear homoleptic aryl derivative was characterized, exhibiting a very short Ag−Ag contact (2.733 Å).[19] A variety of silver clusters were presented from the reaction between deprotonated acetylenes and silver coordination compounds.[20−21] In reactions with sulfur-, selenium-, or tellurium-bearing ligands, many polynuclear silver aggregates were characterized. However, the silver−silver distances in these clusters are larger, around 3.0 Å.[22−29]

In tin coordination chemistry, many molecules are known to form tin−transition metal complexes.[30−31] In addition to the metal−tin single-bond coordination, μ_2- and μ_3-bridging coordination modes have also been described, and transition metal clusters have been stabilized with tin ligands.[32−39] Although tin-bearing molecules are prominent ligands, molecules comprising silver−tin bonds are rare, and cluster skeletons consisting of silver and tin only are so far not known.[40−44]

Currently, we are exploring the coordination chemistry of stanna-*closo*-dodecaborate $[SnB_{11}H_{11}]^{2-}$, a nearly icosahedral heteroborate which can be synthesized in high yield following a simple two step procedure.[45] This cluster serves as versatile nucleophile in coordination chemistry and reacts with various transition metal halides to form a metal−tin bond.[46−49] For the first time, coordination of this borate as an ambident ligand was found in ruthenium chemistry. Here the cluster shows a Ru−Sn and a Ru−(H−B)$_3$ coordination mode in bridging position between two metal centers.[50−53] Furthermore, as a ligand in gold chemistry, the heteroborate cluster shows a lot of variability, thus coordinating via the tin atom at one gold atom or bridging two, three, or four gold centers.[54−55] Because we found short gold−gold interatomic distances in these stannaborate coordination compounds, we started to investigate the coordination of the stannaborate with further electrophiles of the coinage metals. Herein, we report the synthesis and structural characterization of four novel silver−tin clusters, together with quantum chemical calculations focused on the chemical bonding, in particular, concerning the role of the stannaborate units, as well as differences between the two different metal atom types Ag and Au.

Experimental Section

General Procedures. All manipulations were carried out under a nitrogen or argon atmosphere in Schlenk glassware; solvents were dried and purified by standard methods and stored under argon; NMR spectra were recorded on a Bruker AC 200 spectrometer (Institut für Anorganische Chemie, Universität zu Köln) and in Tübingen on a Bruker DRX-250 NMR spectrometer equipped with a 5 mm ATM probe head and operating at 200.13 (^{1}H), 80.25 (^{11}B), 101.25 (^{31}P), and 93.25 MHz (^{119}Sn). Chemical shifts are reported in δ values relative to external $BF_3{\cdot}Et_2O$ (^{11}B), 85% aq H_3PO_4 (^{31}P) or $SnMe_4$ (^{119}Sn) using the chemical shift of the solvent ^{2}H resonance frequency; elemental analysis were carried out on a Hekatech EuroEA C,H,N,S,O elemental analyzer (Institut für Anorganische Chemie, Universität zu Köln) and on a Vario EL Analysator (Institut für Anorganische Chemie, Universität Tübingen). Chemicals were purchased commercially, except for $[Bu_3NH]_2[SnB_{11}H_{11}]$ (**1**), $[Bu_3MeN]_2[SnB_{11}H_{11}]$ (**2**), and $[Et_4N]_2[SnB_{11}H_{11}]$ (**3**), which were prepared according to literature methods or modifications thereof.[45]

Preparation of $[Bu_3MeN]_2[\{Ag(SnB_{11}H_{11})(PPh_3)\}_2]$ (4). A mixture of 3 mL of water, 6 mL of acetone, and 34.0 mg (0.2 mmol) of $AgNO_3$ was treated with an acetone solution (5 mL) of 52.5 mg (0.2 mmol) of PPh_3 and, after 15 min of stirring, with a dichloromethane solution (15 mL) of 129.9 mg (0.2 mmol) of $[Bu_3MeN]_2[SnB_{11}H_{11}]$. After the mixture was stirred for 15 min, water was added, and the dichloromethane phase was separated. Crystallization by slow diffusion of hexane into the dichloromethane phase resulted in colorless crystals. Yield: 116 mg of **4** (71%). ^{11}B{^{1}H} NMR (CD_2Cl_2): δ −13.5 (s, 10B, B2−B11), −5.1 (s, 1B, B12). ^{31}P{^{1}H} NMR (CD_2Cl_2, 293 K): δ 9.0 (s). Anal. Calcd for $C_{62}H_{112}Ag_2B_{22}N_2P_2Sn_2$ (1638.53): C, 45.45; H, 6.89; N, 1.71. Found: C, 44.42; H, 6.88; N, 1.45.

(19) Meyer, E. M.; Gambarotta, S.; Floriani, C.; Chiesi-Villa, A.; Guastini, C. *Organometallics* **1989**, *8*, 1067.
(20) Yam, V. W.-W.; Fung, W. K.-M.; Cheung, K.-K. *Organometallics* **1997**, *16*, 2032.
(21) Lin, Y.-Y.; Lai, S.-W.; Che, C.-M.; Cheung, K.-K.; Zhou, Z.-Y. *Organometallics* **2002**, *21*, 2275.
(22) Perez-Lourido, P.; Garcia-Vazquez, J. A.; Romero, J.; Sousa, A.; Block, E.; Maresca, K. P.; Zubieta, J. *Inorg. Chem.* **1999**, *38*, 538.
(23) Corrigan, J. F.; Fenske, D.; Power, W. P. *Angew. Chem.* **1997**, *36*, 1176.
(24) Henkel, G.; Betz, P.; Krebs, B. *Angew. Chem.* **1987**, *26*, 145.
(25) Fenske, D.; Langetepe, T. *Angew. Chem.* **2002**, *41*, 300.
(26) Canales, S.; Crespo, O.; Gimeno, M. C.; Jones, P. G.; Laguna, A.; Silvestru, A. *Inorg. Chim. Acta* **2003**, *347*, 16.
(27) Kanatzidis, M. G.; Huang, S.-P. *Angew. Chem.* **1989**, *28*, 1513.
(28) Zhao, J.; Adcock, D.; Pennington, W. T.; Kolis, J. W. *Inorg. Chem.* **1990**, *29*, 4358.
(29) Schuerman, J. A.; Fronczek, F. R.; Selbin, J. *Inorg. Chim. Acta* **1989**, *160*, 43.
(30) Petz, W. *Chem. Rev.* **1986**, *86*, 1019.
(31) Holt, M. S.; Wilson, W. L.; Nelson, J. H. *Chem. Rev.* **1989**, *89*, 11.
(32) Simon-Manso, E.; Kubiak, C. P. *Angew. Chem.* **2005**, *44*, 1125.
(33) McNeese, T. J.; Wreford, S. S.; Tipton, D. L.; Bau, R. *Chem. Commun.* **1977**, 390.
(34) Adams, R. D.; Captain, B.; Smith, J. L., Jr. *Inorg. Chem.* **2004**, *43*, 7576.
(35) Breedlove, B. K.; Fanwick, P. E.; Kubiack, C. P. *Inorg. Chem.* **2002**, *41*, 4306.
(36) Garlaschelli, L.; Greco, F.; Peli, G.; Manassero, M.; Sansoni, M.; Della Pergola, R. *Dalton. Trans.* **2003**, 4700.
(37) Jennings, M. C.; Schoettel, G.; Roy, S.; Puddephatt, R. J. *Organometallics* **1991**, *10*, 580.
(38) Zebrowski, J. P.; Hayashi, R. K.; Dahl, L. F. *J. Am. Chem. Soc.* **1993**, *115*, 1142.
(39) Kesanli, B.; Fettinger, J.; Gardner, D. R.; Eichhorn, B. *J. Am. Chem. Soc.* **2002**, *124*, 4779.
(40) Ayers, A. E.; Dias, H. V. R. *Inorg. Chem.* **2002**, *41*, 3259.
(41) Dias, H. V. R.; Ayers, A. *Polyhedron* **2002**, *21*, 611.
(42) Barrow, M.; Bürgi, H.-B.; Camalli, M.; Caruso, F.; Fischer, E.; Venanzi, L. M.; Zambonelli, L. *Inorg. Chem.* **1983**, *22*, 2356.
(43) Findeis, B.; Gade, L. H.; Scowen, I. J.; McPartlin, M. *Inorg. Chem.* **1997**, *36*, 960.
(44) Hitchcock, P. B.; Lappert, M. F.; Piersens, L. J.-M. *Organometallics* **1998**, *17*, 2686.
(45) Chapman, R. W.; Kester, J. G.; Folting, K.; Streib, W. E.; Todd, L. J. *Inorg. Chem.* **1992**, *31*, 979.
(46) Gädt, T.; Wesemann, L. *Organometallics* **2007**, *26*, 2474.
(47) (a) Marx, T.; Mosel, B.; Pantenburg, I.; Hagen, S.; Schulze, H.; Wesemann, L. *Chem.—Eur. J.* **2003**, *9*, 4472. (b) Hagen, S.; Marx, T.; Pantenburg, I.; Wesemann, L.; Nobis, M.; Drie*β*en-Hölscher, B. *Eur. J. Inorg. Chem.* **2002**, 2261.
(48) Marx, T.; Wesemann, L.; Dehnen, S.; Pantenburg, I. *Chem.—Eur. J.* **2001**, *7*, 3025.
(49) Wesemann, L.; Marx, T.; Englert, U.; Ruck, M. *Eur. J. Inorg. Chem.* **1999**, *9*, 1563.
(50) Gädt, T.; Grau, B.; Eichele, K.; Pantenburg, I.; Wesemann, L. *Chem.—Eur. J.* **2006**, *12*, 1036.
(51) Gädt, T.; Wesemann, L. *Dalton Trans.* **2006**, 328.
(52) Gädt, T.; Eichele, K.; Wesemann, L. *Dalton. Trans.* **2006**, 2706.
(53) Gädt, T.; Eichele, K.; Wesemann, L. *Organometallics* **2006**, *25*, 3904.
(54) Hagen, S.; Pantenburg, I.; Weigend, F.; Wickleder, C.; Wesemann, L. *Angew. Chem.* **2003**, *42*, 1501.
(55) Hagen, S.; Wesemann, L.; Pantenburg, I. *Chem. Commun.* **2005**, 1013.

Scheme 1. Formation of the Dimer $[\{Ag(SnB_{11}H_{11})(PPh_3)\}_2]^{2-}$ (Dianion of **4**)

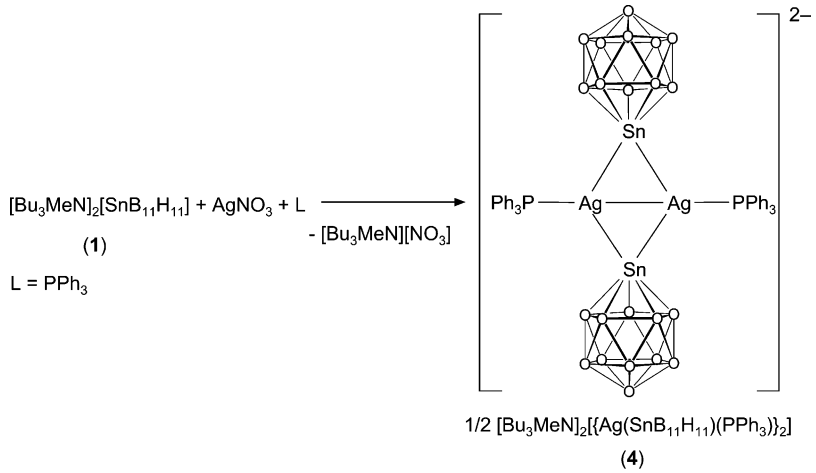

Scheme 2. Formation of the Trimer $[\{Ag(SnB_{11}H_{11})(PEt_3)\}_3]^{3-}$ (Trianion of **5**)

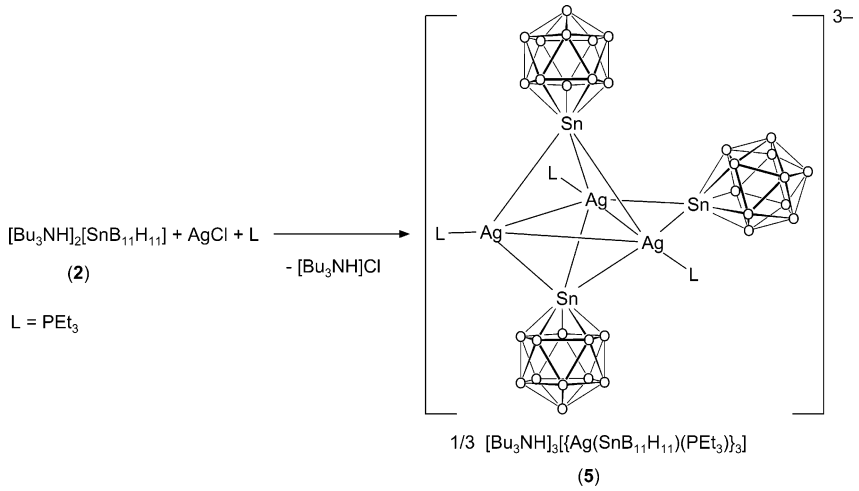

Scheme 3. Formation of the Tetramer $[\{Ag(SnB_{11}H_{11})(PMe_3)\}_4]^{4-}$ (Tetraanion of **6**)

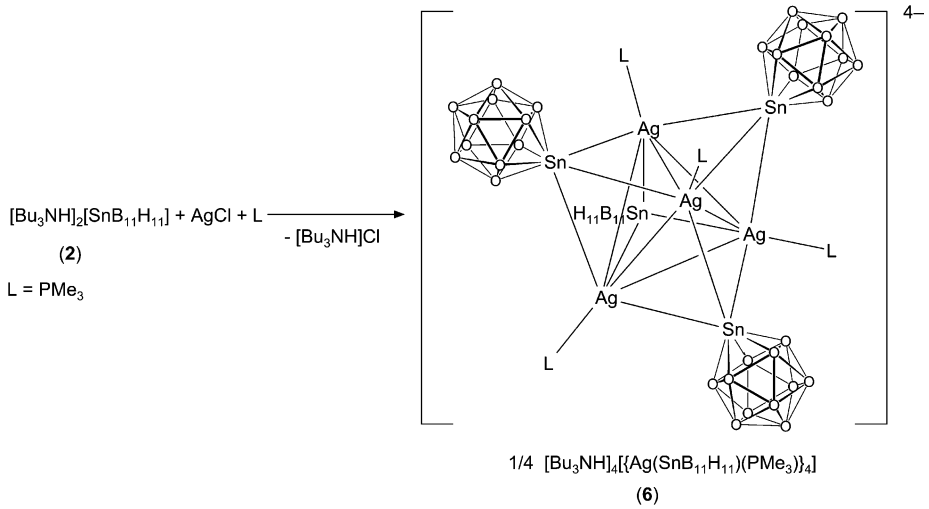

Preparation of $[Bu_3NH]_3[\{Ag(SnB_{11}H_{11})(PEt_3)\}_3]$ (5). A suspension of AgCl (28.7 mg, 0.2 mmol) and 7 mL of benzene was treated at room temperature with 29 μL of PEt_3 (0.2 mmol). After the mixture was stirred for 20 h, the colorless solution was reacted with 124.3 mg of $[Bu_3NH]_2[SnB_{11}H_{11}]$ (0.2 mmol) dissolved in 15 mL of dichloromethane. After it was stirred for 30 min, the dichloromethane mixture was washed several times with water. The reaction product was dried under vacuum and crystallized by slow diffusion of hexane into a dichloromethane solution. Yield of **5**: 127 mg (88%) of colorless crystals. $^{11}B\{^1H\}$ NMR (CD_2Cl_2): δ −13.4 (s, 10B, B2−B11), −4.7 (s, 1B, B12). $^{31}P\{^1H\}$ NMR (CD_2Cl_2, 293 K): δ 8.7 (s). Anal. Calcd for $C_{54}H_{162}Ag_3B_{33}N_3P_3Sn_3$ (1983.32): C, 32.70; H, 8.23; N, 2.12. Found: C, 32.07; H, 8.07; N, 1.80.

Preparation of $[Bu_3NH]_4[\{Ag(SnB_{11}H_{11})(PMe_3)\}_4]$ (6). A suspension of AgCl (28.7 mg, 0.2 mmol) and 7 mL of benzene

Table 1. Crystal Data and Summary of Data Collection and Refinement for Compounds $[Bu_3MeN]_2[\{Ag(SnB_{11}H_{11})(PPh_3)\}_2]$ (**4**), $[Bu_3NH]_3[\{Ag(SnB_{11}H_{11})(PEt_3)\}_3]$ (**5**), $[Bu_3NH]_4[\{Ag(SnB_{11}H_{11})(PMe_3)\}_4]$ (**6**), and $[Et_4N]_8[Ag_4(SnB_{11}H_{11})_6]$ (**7**)

	4	**5** × $^1/_2CH_2Cl_2$	**6**	**7** × $7CH_3CN$
formula	$C_{62}H_{112}Ag_2B_{22}N_2P_2Sn_2$	$C_{54.5}H_{162}Ag_3B_{33}ClN_3P_3Sn_3$	$C_{60}H_{192}Ag_4B_{44}N_4P_4Sn_4$	$C_{78}H_{247}Ag_4B_{66}N_{15}Sn_6$
fw (g mol^{-1})	1638.42	2024.64	2475.94	3252.99
space group	triclinic, $P\bar{1}$ (No. 2)	triclinic, $P\bar{1}$ (No. 2)	monoclinic, $C2/c$ (No. 15)	triclinic, $P\bar{1}$ (No. 2)
a (Å)	11.607(1)	15.7176(17)	23.678(2)	17.9477(8)
b (Å)	12.855(1)	16.8227(15)	40.503(3)	18.5844(8)
c (Å)	14.734(1)	21.692(2)	16.682(2)	23.6049(9)
α (deg)	68.158(6)	99.861(8)		91.685(3)
β (deg)	75.747(7)	97.800(8)	135.054(6)	100.181(3)
γ (deg)	71.529(6)	116.129(7)		97.343(4)
Z/vol (Å^3)	1/1914.9(3)	2 / 4926.8(8)	4/11302.0(18)	2/7674.9(6)
T (K)	130	173	170	173
collected/unique/observed	34 928/8413/7788	60 415/20 594/12 343	70 477/10 011/5405	14 1711/41 767/28 618
R_{merg}	0.0789	0.1221	0.1178	0.0738
R indexes [$I > 2\sigma(I)$]	R1 = 0.0265 wR2 = 0.0673	R1 = 0.0884 wR2 = 0.1161	R1 = 0.0612 wR2 = 0.1297	R1 = 0.0514 wR2 = 0.0958
R indexes (all data)	R1 = 0.0292 wR2 = 0.0684	R1 = 0.1590 wR2 = 0.1345	R1 = 0.1197 wR2 = 0.1457	R1 = 0.0932 wR2 = 0.1141

was treated at room temperature with 20 μL of PMe_3 (0.2 mmol). After it was stirred for 20 h, the colorless solution was reacted with 124.3 mg of $[Bu_3NH]_2[SnB_{11}H_{11}]$ (0.2 mmol) dissolved in 15 mL of dichloromethane. After it was stirred for 30 min, the dichloromethane mixture was washed several times with water. The reaction product was dried under vacuum and crystallized by slow diffusion of hexane into a dichloromethane solution. Yield of **6**: 105 mg (85%) of pale-yellow crystals. $^{11}B\{^1H\}$ NMR (CD_2Cl_2): δ −13.4 (s, 10B, B2−B11), −4.7 (s, 1B, B12). $^{31}P\{^1H\}$ NMR (CD_2Cl_2, 293 K): δ −34.5 (s). Anal. Calcd for $C_{60}H_{192}Ag_4B_{44}N_4P_4Sn_4$ (2476.10): C, 29.10; H, 7.82; N, 2.26. Found: C, 28.86; H, 8.06; N, 2.06.

Preparation of $[Et_4N]_8[Ag_4(SnB_{11}H_{11})_6]$ (7). A solution of 13 mg $AgNO_3$ (0.08 mmol) in 10 mL of acetonitrile was treated with an acetonitrile solution (10 mL) of 61.1 mg (0.12mmol) of $[Et_4N]_2[SnB_{11}H_{11}]$. After filtration through Celite, green crystals were obtained by slow diffusion of diethylether into the acetonitrile phase at +4 °C. Yield of **7**: 43 mg (72%) of green crystals. $^{11}B\{^1H\}$ NMR (CD_3CN): δ −12.1 (s, 10B, B2−B11), −2.8 (s, 1B, B12). ^{119}Sn NMR (CD_3CN): δ −416 (s). Anal. Calcd for $C_{64}H_{226}Ag_4B_{66}N_8Sn_6$ (2965.81): C, 25.92; H, 7.68; N, 3.78. Found: C, 25.38; H, 7.62; N, 3.70.

X-ray Structure Determination. X-ray data for compounds **4** and **6** were collected on a Stoe IPDS 2 and for **5** and **7** on a Stoe IPDS 2T diffractometer, and they were corrected for Lorentz and polarization effects and absorption by air. Numerical absorption

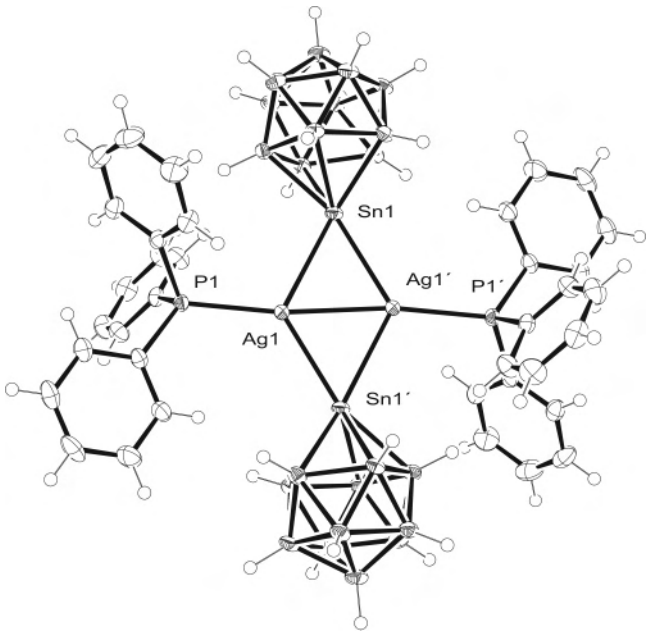

Figure 1. Molecular structure of the dianion of **4**. Selected bond distances (Å) and angles (deg): Ag1−Ag1′ = 2.7160(4), Ag1−Sn1 = 2.8216(4), Ag1′−Sn1 = 2.7607(4), Ag1−P1 = 2.4527(6), Ag1−Sn1−Ag1′ = 58.215(9), Sn1−Ag1−Sn1′ = 121.785(9), P1−Ag1−Ag1′ = 171.739(18).

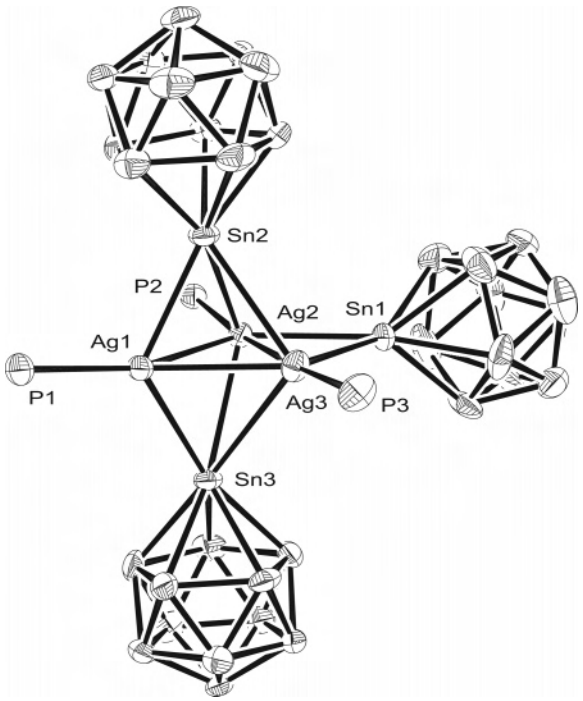

Figure 2. Molecular structure of the trianion of **5**. Ethyl substituents at the phosphorus atoms and hydrogen atoms at the boron atoms have been omitted for clarity. Selected bond distances (Å) and angles (deg): Ag2−Ag1 = 2.8356(10), Ag3−Ag1 = 2.9091(11), Ag2−Ag3 = 2.6326(10), Sn1−Ag2 = 2.7801(10), Sn1−Ag3 = 2.8303(11), Ag1−Sn2 = 2.7649(10), Ag1−Sn3 = 2.7651(10), Ag2−Sn2 = 2.9434(10), Ag2−Sn3 = 2.9614(10), Ag3−Sn2 = 2.9900(11), Ag3−Sn3 = 3.1269(11), Ag1−P1 = 2.434(2), Ag2−P2 = 2.393(3), Ag3−P3 = 2.392(3), Ag2−Sn1−Ag3 = 55.96(2), Ag1−Sn2−Ag2 = 59.47(2), Ag1−Sn2−Ag3 = 60.58(3), Ag2−Sn2−Ag3 = 52.67(2), Ag1−Sn3−Ag2 = 59.24(2), Ag1−Sn3−Ag3 = 58.79(3), Ag2−Sn3−Ag3 = 51.15(2), Sn2−Ag1−Sn3 = 121.74(3), P1−Ag1−Ag2 = 156.50(8), P1−Ag1−Ag3 = 146.48(8), Ag2−Ag1−Ag3 = 54.53(2), P2−Ag2−Ag3 = 173.43(7), Ag3−Ag2−Ag1 = 64.16(3), P3−Ag3−Ag2 = 176.24(8), Ag2−Ag3−Ag1 = 61.31(3).

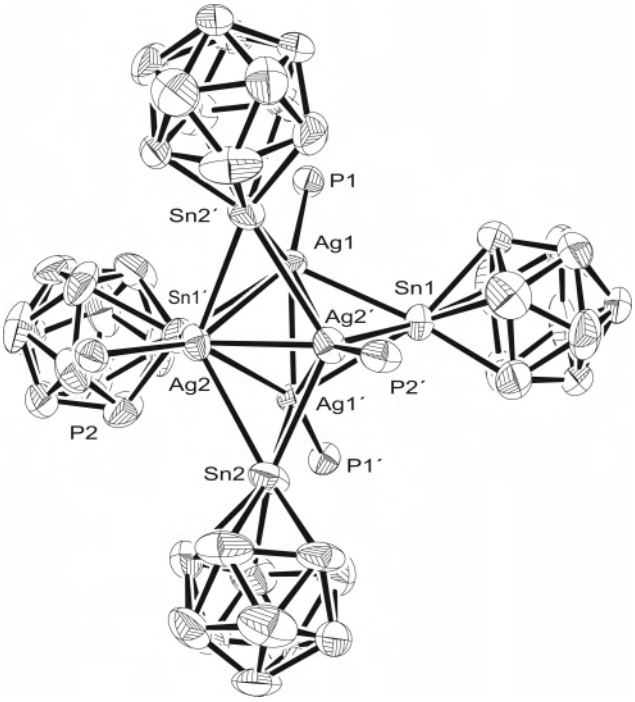

Figure 3. Molecular structure of the tetraanion of **6**. Methyl substituents at the phosphorus atoms and hydrogen atoms at the boron atoms have been omitted for clarity.

correction based on crystal−shape optimization was applied for **4** and **6**. The programs used in this work are Stoe's X-Area[56] and the WinGX suite of programs[57] including SHELXS and SHELXL[58] for structure solution and refinement.

Results and Discussion

Syntheses and Solid-State Structures. Ever since we isolated novel Au−Sn clusters with short Au−Au interactions, from the reaction of the stannaborate with gold(I) electrophiles, we were very much interested in the analogous silver chemistry. Here we present our results on the reaction of different phosphine silver electrophiles $[Ag(PR_3)]^+$ (PR_3 = PPh_3, PEt_3, PMe_3) with the nucleophilic tin ligand $[SnB_{11}H_{11}]^{2-}$. Furthermore, the product of the reaction of $AgNO_3$ and $[SnB_{11}H_{11}]^{2-}$ without the presence of a coligand is presented.

The reactions were carried out at room temperature, and the novel silver−tin coordination compounds were purified by crystallization and characterized by elemental analyses, X-ray crystal structure analyses, and NMR spectroscopy.

From the reaction of the monophosphine electrophiles $[Ag(PR_3)]^+$ with 1 equiv of the tin heteroborate, we found formation of silver−stannaborate aggregates with tin−metal coordination of different size and of general formula

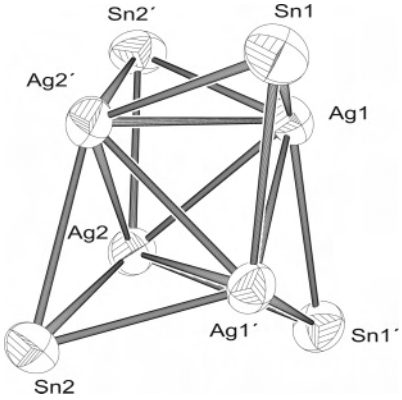

Figure 4. Cluster core of the tetraanion of **6**. Selected bond distances (Å): Ag1−Ag1′ = 2.7941(13), Ag1−Ag2 = 2.9320(10), Ag1−Ag2′ = 2.9450(10), Ag2−Ag2′ = 2.7841(15), Ag1−Sn1 = 2.9087(10), Ag1−Sn2′ = 2.8081(10), Ag1−Sn1′ = 3.0592(11), Ag2−Ag1′ = 2.9450(10), Ag2−Sn1′ = 2.8258(10), Ag2−Sn2′ = 2.9451(11), Ag2−Sn2 = 3.1198(11), Ag1−P1 = 2.449(2), Ag2−P2 = 2.439(3).

$[\{Ag(SnB_{11}H_{11})(PR_3)\}_n]^{n-}$, namely, a dimer (**4**) in the case of triphenylphosphine (PPh_3, $n = 2$; Scheme 1), a trimer (**5**) (PEt_3, $n = 3$, Scheme 2), and a tetramer (**6**) (PMe_3, $n = 4$, Scheme 3). The structures of these novel silver−tin clusters were determined by single-crystal X-ray structure analyses. Suitable crystals of **4**, **5**, and **6** were obtained by slow diffusion of hexane into a dichloromethane solution of the respective salts. Details of the crystal structure analyses are listed in Table 1, and drawings of the cluster anions of **4**, **5**, and **6** are depicted in Figures 1−4.

Only three other types of tin(II) nucleophiles are known to form silver−tin bonds in reaction with silver electrophiles: a lithium triamidostannate $[MeSi\{SiMe_2N(p\text{-}Tol)\}_3SnLi(OEt_2)]$,[43] a dialkylstannylene $[Sn\{CH(SiMe_3)_2\}_2]$,[44] and tin(II) aminotroponiminate complexes.[40,41]

We found a dependence of the nuclearity of the silver−tin cluster on the cone angle (Ph_3P, 145°; Et_3P, 132°; Me_3P, 118°): the smaller the phosphine, the higher the nuclearity of the cluster. The geometries of the dimer (**4**) and the trimer (**5**) correspond to the homologous gold compounds $[Bu_3NH]_2[\{Au(SnB_{11}H_{11})(PPh_3)\}_2]$ and $[Bu_3NH]_3[\{Au(SnB_{11}H_{11})(PEt_3)\}_3]$.[54,55] As expected from the observations made by Schmidbaur that the covalent radius of gold(I) is smaller than that of silver(I), the Ag−Ag, Ag−P, and Ag−Sn interatomic distances are slightly longer than the corresponding Au−Au, Au−P, and Au−Sn distances (Table 2).[59,60]

Like in the gold-cluster structure, the tin ligand shows a μ_2-bridging coordination mode in silver compound **4**. The Ag−Ag interatomic distance of 2.7160(4) Å in **4** is shorter than the Ag−Ag distance in metallic silver, 2.89 Å, and the Ag−Ag interaction in many other element-bridged Ag−E−

Table 2. Comparison of Selected Interatomic Distances (Å) in Analogous Ag and Au Dimers, **4** and $[Bu_3NH]_2[\{Au(SnB_{11}H_{11})(PPh_3)\}_2]$, and Trimers, **5** and $[Bu_3NH]_3[\{Au(SnB_{11}H_{11})(PEt_3)\}_3]$ (see Figure 5)

	4		Au-dimer		**5**		Au-trimer	
M−M	Ag−Ag	2.7160(4)	Au−Au	2.625(1)	Ag2−Ag3	2.6326(10)	Au2−Au3	2.605(1)
					Ag1−Ag2	2.8356(10)	Au1−Au2	2.793(1)
					Ag1−Ag3	2.9091(11)	Au1−Au3	2.894(1)
M−Sn	Ag−Sn	2.8216(4), 2.7607(4)	Au−Sn	2.761(1), 2.737(1)	Ag2−Sn1	2.7801(10)	Au2−Sn1	2.735(1)
					Ag3−Sn1	2.8303(11)	Au3−Sn1	2.811(1)
M−P	Ag−P	2.4527(6)	Au−P	2.332(1)	Ag1−P1	2.434(2)	Au1−P1	2.314(2)
					Ag2−Sn2	2.393(2)	Au2−*P2*	2.299(2)

Scheme 4. Formation of a Tetranuclear Silver Cluster **7** without Supporting Ligand

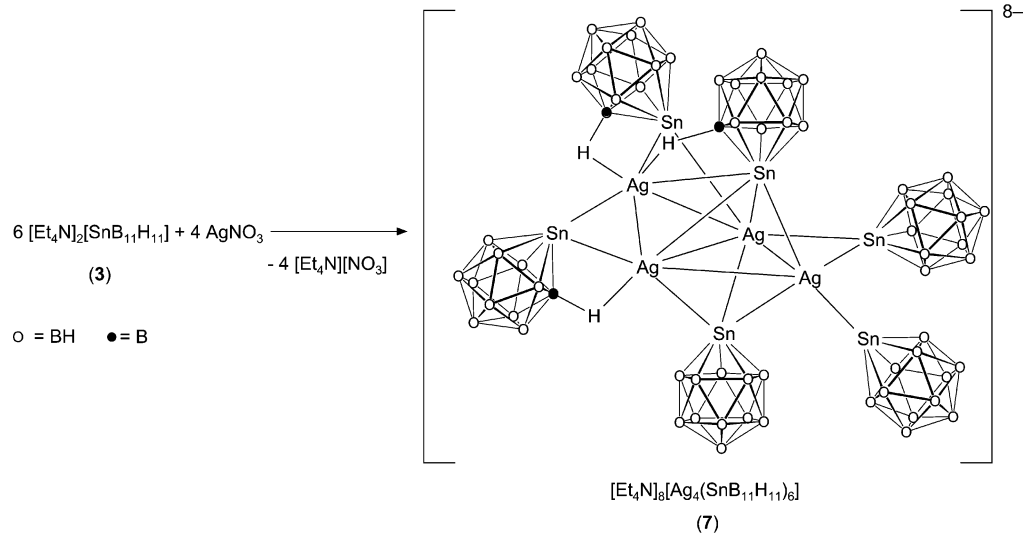

Ag structures: E = SPh, 2.991 Å;[61] E = I, 2.977 Å;[62] E = AsPh, 2.885 Å;[63] E = C(carbene), 2.780 Å,[17−18] C(phenyl), 2.733 Å.[19] An interesting example for a shorter Ag−Ag distance of 2.6544 Å was found in the heterobimetallic tin−silver complex $[MeSi\{SiMe_2N(p\text{-Tol})\}_3SnAg]_2$.[43] The Ag−Sn interatomic distances of 2.8216(4) and 2.7607(4) Å in **4** are longer than the reported values in the literature (2.5863−2.6567 Å).[40−44]

In the trinuclear silver-cluster **5**, two of the three stannaborate moieties show a μ_3-bridging coordination mode, and one is coordinated in a μ_2-bridging fashion. The silver−tin distances range between 2.7649(10) and 3.1269(11) Å. In the silver triangle, the silver−silver edge, Ag2−Ag3 (Figure 2), bridged by a μ_2-coordinating ligand exhibits a short Ag−Ag contact of 2.6326(10) Å. To our knowledge, this is one of the shortest Ag−Ag contacts in silver coordination compounds.

In the reaction with trimethylphosphine, we found a tetranuclear silver cluster **6** (Figures 3 and 4) with the stannaborate coordinated in a face-bridging mode at the triangles of the silver tetrahedron. The molecular structure of the tetraanion and the cluster core are shown in Figures 3 and 4. The cluster lies on a two-fold axis of rotation, and therefore, only four independent Ag−Ag interatomic distances in the range of 2.7841(15)−2.9450(10) Å are found. In the series of structurally characterized silver tetrahedrons with various bridging ligands, the presented example exhibits the shortest averaged Ag−Ag interatomic distances.[24−29] Because the tin ligand is μ_3-coordinated at the silver tetrahedron, the Ag−Sn interatomic distances are relatively long and vary between 2.8081(10) and 3.1198(11) Å.

From the reaction of $AgNO_3$ with stanna-*closo*-dodecaborate without a supporting phosphine ligand, we were able to isolate, in good yield, green crystals of an octaanionic coordination compound consisting of four silver cations and six stannaborate dianions (Scheme 4). The molecular structure of the anion is shown in Figure 6, and the cluster core is depicted in Figure 7. Details of the crystal structure determination of **7** are listed in Table 1.

The four silver atoms are arranged in a butterfly-type Ag_4 cluster with a torsional angle Ag4−Ag2−Ag1−Ag3 of 146.9°. The Ag−Ag interatomic distances are in a range of 2.7102(5)−3.1424(6) Å, with the Ag4 silver atom showing the longest contacts to Ag1 and Ag2. As in the structure of the trimer **5**, the Ag1−Ag3 cluster edge bridged by a μ_2-coordinating stannaborate exhibits the shortest distance. Interestingly, the six heteroborate ligands display five different coordination modes in the structure of **7**. The stannaborate moiety with tin atom Sn4 shows η^1-coordination at the coinage metal (here, Ag3) and therefore a short Ag−Sn bond length of 2.6416(5) Å. As already described for the related compounds **4**−**6**, the stannaborates with Sn1 and Sn6 show μ_2- and μ_3-coordination, respectively. A so far unknown coordination mode is presented for the cluster with Sn2: the heteroborate exhibits four tin−silver contacts together with a B−H unit η^1-coordinated at Ag4 [B201−Ag4 = 2.798(6) Å]. A closely related type of coordination

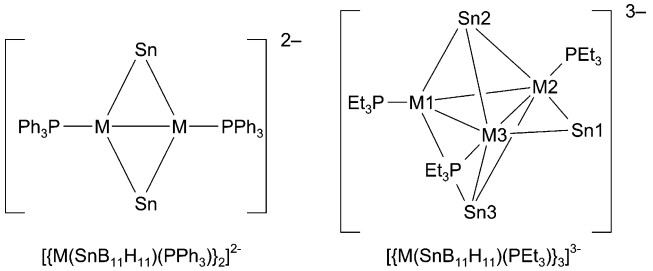

Figure 5. Geometries of the analogous silver and gold clusters.

(56) *X-AREA*, version 1.26; Stoe & Cie GmbH: Darmstadt, Germany, 2004.
(57) Farrugia, L. J. *J. Appl. Crystallogr.* **1999**, *32*, 837.
(58) (a) Sheldrick, G. M. *SHELXS-97, Program for the Solution of Crystal Structures*; University of Göttingen: Göttingen, Germany, 1997. (b) Sheldrick, G. M. *SHELXL-97, Program for Crystal Structure Refinement*; University of Göttingen: Göttingen, Germany, 1997.
(59) Tripathi, U. M.; Bauer, A.; Schmidbaur, H. *Dalton. Trans.* **1997**, 2865.
(60) Fernández, E. F.; López-de-Luzuriaga, J. M.; Monge, M.; Rodríguez, A. M.; Crespo, O.; Gimeon, M. C.; Laguna, A.; Jones, P. G. *Inorg. Chem.* **1998**, *37*, 6002, 6006.
(61) Wang, X.-J.; Langtepe, T.; Fenske, D.; Kang, B.-S. *Z. Anorg. Allg. Chem.* **2002**, *628*, 1158.
(62) Bowmaker, G. A.; Effendy; Harvey, P. J.; Healy, P. C.; Skelton, B. W.; White, A. H. *Dalton Trans.* **1996**, 2459.
(63) Fenske, D.; Simon, S. *Z. Anorg. Allg. Chem.* **1996**, *622*, 45.

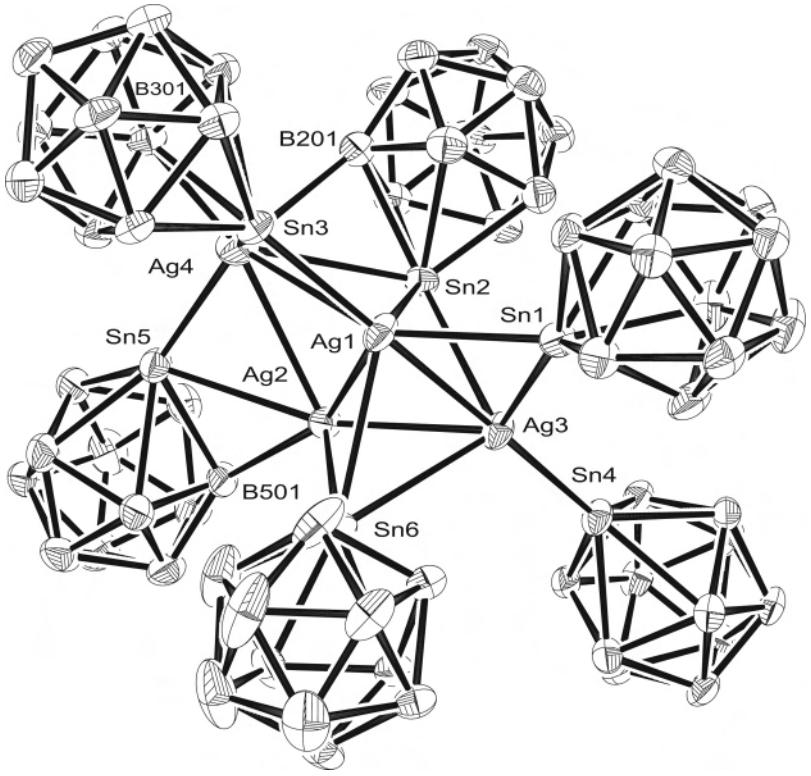

Figure 6. Molecular structure of the octaanion of **7**. Hydrogen atoms at the boron atoms have been omitted for clarity.

mode is realized for the ligands with Sn3 and Sn5. Here the μ_2-coordination of the tin atom and η^1(B−H)-coordination at silver [B301−Ag4 = 2.740(6) Å, B501−Ag2 = 2.651(6) Å] is found, presenting further examples for the versatile coordination capabilities of the dianion $[SnB_{11}H_{11}]^{2-}$. The (B−H)-coordination of boranes is well-known in the literature.[64] Recently, we have presented examples for the ambident coordination mode of the stanna-*closo*-dodecaborate ligand in ruthenium and iron coordination chemistry: η^3-(B−H)-M (M = Ru, Fe) together with η^1(Sn)-M (M = Ru, Cr, Mo, W).[50−53]

We also tried to explore the new silver coordination compounds by NMR spectroscopy in solution. In the ^{11}B NMR spectrum, signals around −5 (1B) and −13 (10B) ppm are a good proof of coordination of the heteroborate at the silver electrophiles [^{11}B NMR of uncoordinated $SnB_{11}H_{11}$: δ −5.1(1B), −10.6(5B), −11.9(5B)]. The ^{31}P NMR spectra of the respective phosphine complexes **4**, **5**, and **6** exhibit, in each case, a relatively broad single signal at room temperature. We interpret the missing splitting as being the result of P−Ag couplings and the absence of tin satellites in these spectra as an indicator for dynamic behavior of the cluster anions in solution. Recording the ^{31}P NMR spectra at −60 °C resulted in the observation of a broad doublet, giving no further information about the structure of the anions in solution. Because of solubility problems, we were not able to measure NMR spectra at lower temperatures. In the case of the cluster salt **7**, a signal at −416 in the ^{119}Sn NMR spectrum confirms coordination of the stannaborate in

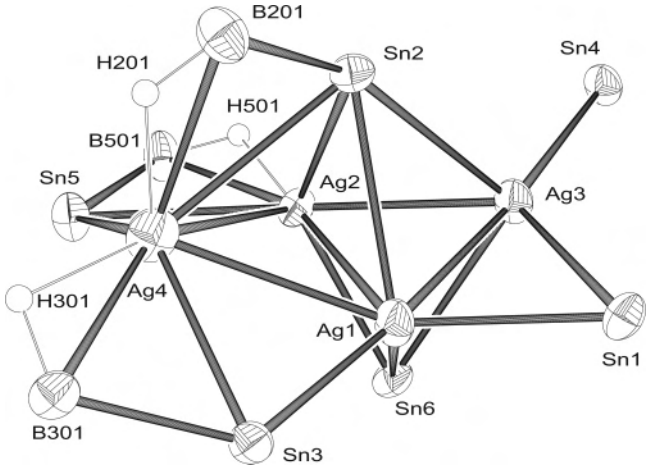

Figure 7. Cluster core of the octaanion of **7**. Only boron atoms involved in B−H−Ag three-center two-electron bonds are shown. Selected bond distances (Å) and angles (deg): Ag1−Ag3 = 2.7102(5), Ag1−Ag2 = 2.8665(5), Ag1−Ag4 = 3.1424(6), Ag2−Ag3 = 2.8762(5), Ag2−Ag4 = 3.1326(6), Sn1−Ag3 = 2.7806(5), Sn1−Ag1 = 2.7807(5), Sn2−Ag2 = 2.7878(5), Sn2−Ag3 = 3.0622(5), Sn2−Ag1 = 3.0944(5), Sn2−Ag4 = 3.1460(6), Sn3−Ag1 = 2.6445(5), Sn3−Ag4 = 2.8923(5), Sn4−Ag3 = 2.6416(5), Sn5−Ag4 = 2.6665(6), Sn5−Ag2 = 2.9644(5), Sn6−Ag2 = 2.7515(5), Sn6−Ag1 = 3.0209(6), Sn6−Ag3 = 3.1149(6), B301−Ag4 = 2.740(6), B501−Ag2 = 2.651(6), B201−Ag4 = 2.798(6), Ag3−Sn1−Ag1 = 58.331(13), Ag1−Sn3−Ag4 = 68.992(15), Ag4−Sn5−Ag2 = 67.364-(15), Sn3−Ag1−Ag3 = 175.40(2), Ag3−Ag1−Ag4 = 116.194(17), Ag3−Ag2−Ag4 = 111.664(16), Sn4−Ag3−Ag1 = 174.71(2).

(64) (a) Ellis, D. D.; Jelliss, P. A.; Stone, F. G. A. *Organometallics* **1999**, *18*, 4982. (b) Pisareva, I. V.; Konoplev, V. E.; Petrovskii, P. V.; Vorontsov, E. V.; Dolgushin, F. M.; Yanovsky, A. I.; Chizhevsky, I. T. *Inorg. Chem.* **2004**, *43*, 6228. (c) Hodson, B. E.; McGrath, T. D.; Stone, F. G. A. *Organometallics* **2005**, *24*, 1638. (d) Hodson, B. E.; McGrath, T. D.; Stone, F. G. A. *Dalton Trans.* **2004**, 2570. (e) Teixidor, F.; Nuñez, R.; Flores, M. A.; Demonceau, A.; Viñas, C. *J. Organomet. Chem.* **2000**, *614−615*, 48. (f) Viñas, C.; Nuñez, R.; Teixidor, F.; Kivekäs, R.; Sillanpäa, R. *Organometallics* **1996**, *15*, 3850. (g) Patmore, N. J.; Hague, C.; Cotgreave, J. H.; Mahon, M. F.; Frost, C. G.; Weller, A. S. *Chem.−Eur. J.* **2002**, *8*, 2088.

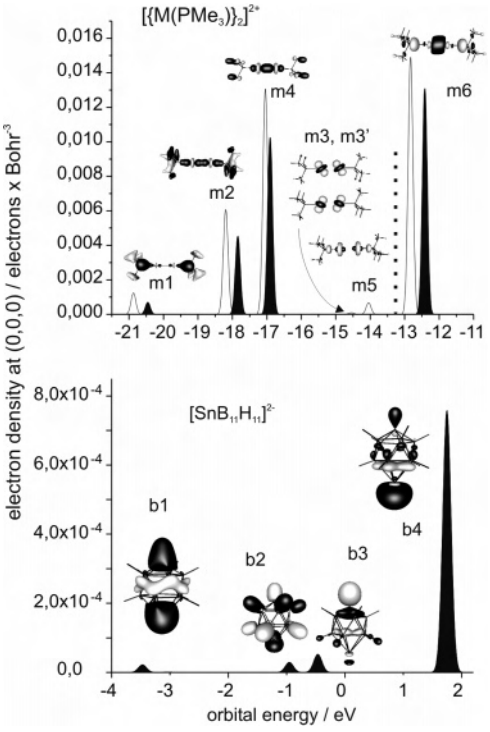

Figure 8. Orbital contributions to the electron density at the molecular center (0,0,0) versus orbital energies for $[\{M(PMe_3)\}_2]^{2+}$, upper panel, filled area under the curve in case of Ag, non-filled for Au, and $[SnB_{11}H_{11}]_2^{2-}$, lower panel. Lines are broadened to help the eye. Surfaces of contour plots of relevant orbitals are drawn at amplitude values of ±0.05 (electrons/Bohr^3)$^{1/2}$; in the upper panel, contour plots of orbitals refer to M = Au, and those for M = Ag are very similar. The dotted line in the upper panel separates occupied orbitals m1−m5 from unoccupied m6.

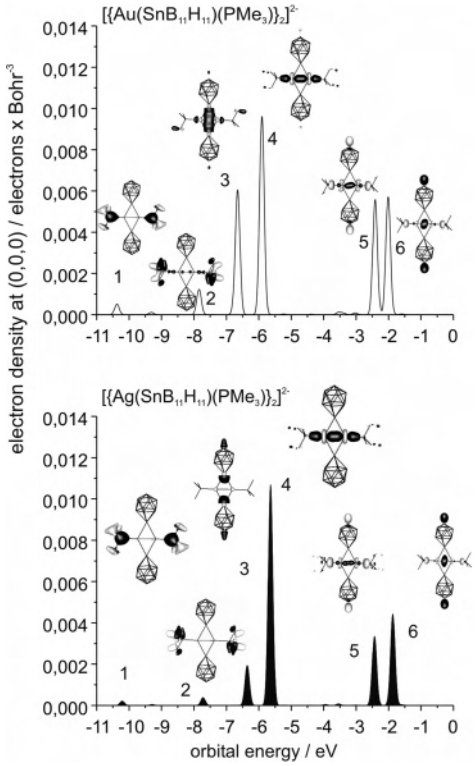

Figure 9. Orbital contributions to the electron density at the molecular center versus orbital energies for $[\{M(SnB_{11}H_{11})(PMe_3)\}_2]^{2-}$ (upper panel: M = Au, lower panel: M = Ag). See also Figure 8.

solution because the uncoordinated ligand has a ^{119}Sn chemical shift of −546 ppm.

Quantum Chemical Investigations. The focus of our quantum chemical calculations was the role of the stannaborate units and the differences in chemical bonding for the two different metal atom types Ag and Au. Similarities and differences were studied in detail for $[\{M(SnB_{11}H_{11})(PMe_3)\}_2]^{2-}$, M = Ag, Au; larger systems **5**−**6** are briefly discussed at the end. Methods of density functional theory were employed using functional B-P86,[65,66] basis sets of type def2-TZVP[67] plus corresponding RI-J auxiliary basis sets,[68] in connection with effective core potentials for Au, Ag,[69] and Sn.[70] For M = Au, it was demonstrated previously[54] that DFT yields qualitatively correct results for these systems. At that time, it was found, that in the Au dimer, Au−Au distances were overestimated by 3 pm, and Au−Sn distances were overestimated by ∼10 pm. It was also discovered that errors at the HF level are much larger (+10 pm for Au−Au and +20 pm for Au−Sn), while MP2 equilibrium distances are practically identical with experimental data. Comparison of MP2 and HF data indicates a large influence of dynamic electron correlation, probably due to dispersive interactions, which are important for a quantitatively accurate description of the entire systems. Nevertheless, for a qualitative understanding of the role of the stannaborates DFT results are sufficient.

Let us regard $[\{M(SnB_{11}H_{11})(PMe_3)\}_2]^{2-}$ as a $[\{M(PMe_3)\}_2]^{2+}$ cation coordinated by two anionic $[SnB_{11}H_{11}]^{2-}$ units. We start with the bare $[\{M(PMe_3)\}_2]^{2+}$ cation. Note that for simplicity the phenyl groups were replaced by methyl groups. For reasons of better comparability, the geometric structure of $[\{Ag(SnB_{11}H_{11})(PMe_3)\}_2]^{2-}$ was taken in all cases, and the cationic subsystem was obtained by removing the $[SnB_{11}H_{11}]^{2-}$ units without further structure optimization. Orbitals responsible for the M−M bond are expected to contribute to the electronic density between the two M atoms. Thus, to distinguish relevant from less-relevant orbitals, the electron density (squared amplitude) in the middle of the M−M axis was calculated for each orbital. The respective values are plotted versus the orbital energy for M = Ag, Au in the upper panel of Figure 8. Contour plots of orbitals with significant densities at the molecular center are also provided in Figure 8. One obtains qualitatively similar but quantitatively different pictures for the two metals. In both cases, two binding combinations of (mainly) d_{z^2} orbitals at Ag/Au (z denotes the bond axis between these atoms) are the most important (occupied) orbitals at the M−M bond. These orbitals are labeled m2 and m4: m2 is also bonding with respect to the metal−ligand bond, and m4 is antibonding in that sense and yields the largest contribution. The symmetric combination, m6, of (mainly) s-orbitals of the two metal atoms, shows the highest density at the molecular center, but it is unoccupied for the cationic species and thus does not contribute to the M−M

(65) Perdew, J. P. *Phys. Rev. B* **1986**, *33*, 8822.
(66) Becke, A. D. *J. Chem. Phys.* **1993**, *98*, 5648.
(67) Weigend, F.; Ahlrichs, R. *Phys. Chem. Chem. Phys.* **2005**, *7*, 3297.
(68) Weigend, F. *Phys. Chem. Chem. Phys.* **2006**, *8*, 1057.
(69) Andrae, D.; Haeussermann, U.; Dolg, M.; Stoll, H.; Preuss, H. *Theor. Chim. Acta* **1990**, *77*, 123.
(70) Metz, D.; Stoll, H.; Dolg, M. *J. Chem. Phys.* **2000**, *113*, 2563.

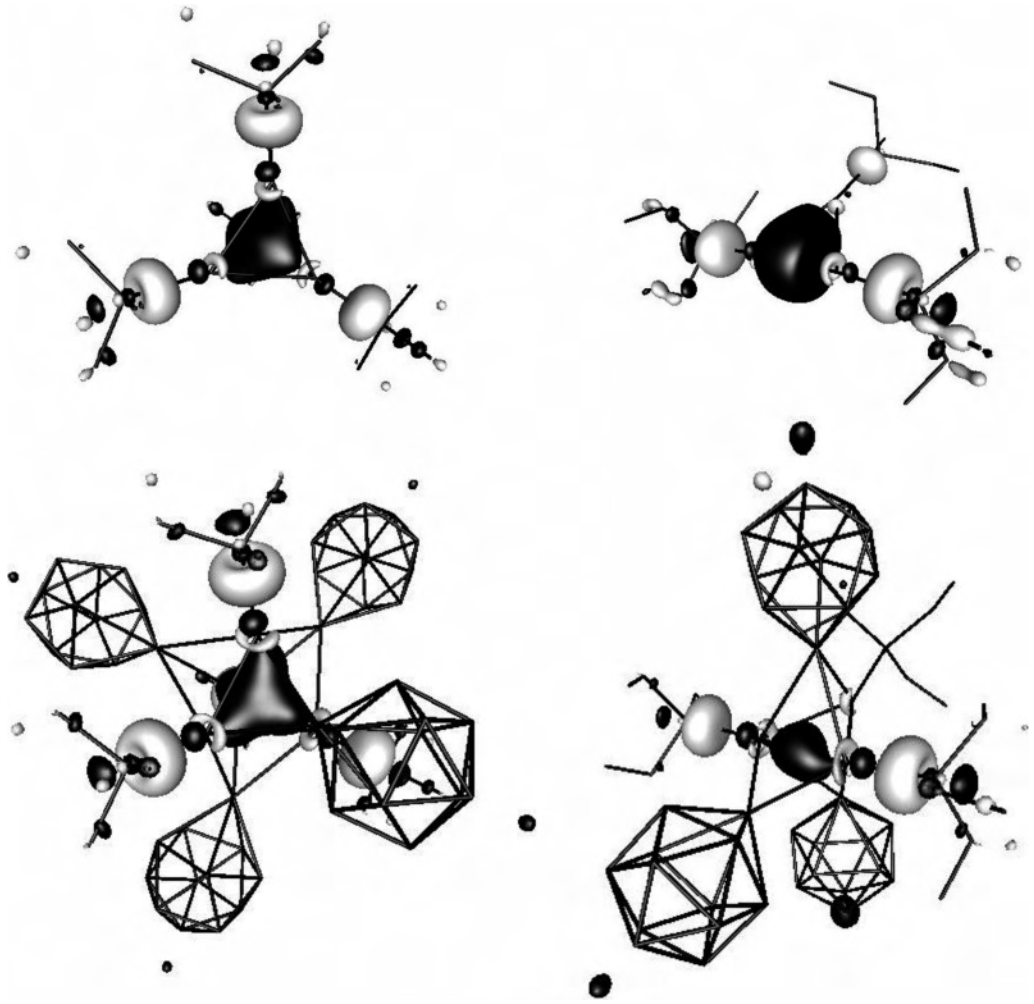

Figure 10. Upper part: LUMOs of the stannaborate-free systems $[\{Ag(PMe_3)\}_4]^{4+}$, left (the fourth methyl group is hidden by the part of the LUMO located in the Ag_4 core), and $[\{Ag(PEt_3)\}_3]^{3+}$, right. Lower part: Corresponding occupied orbitals of the entire compounds $[\{Ag(SnB_{11}H_{11})(PMe_3)\}_4]^{4-}$ and $[\{Ag(SnB_{11}H_{11})(PEt_3)\}_3]^{3-}$ resulting from the respective LUMOs. See also Figures 8 and 9.

bond. Of lower relevance are m1, which is similar to m2, but located at the phosphorus atoms, and m5. The main difference between Ag and Au compounds is a ~30% higher electron density at the molecular center of the Au molecule which can be found by comparing all orbitals. Note that the structure parameters are the same for both cases, so this effect is solely caused by exchange of the coinage metal type. The larger density may be rationalized by relativistic effects allowing for a partial hybridization of the $5d_{z^2}$ and the 6s orbital in the case of Au.[3]

Next we investigated changes in the bonding situation when the stannaborate units were added. The same analysis as above was carried out for the entire system, $[\{M(SnB_{11}H_{11})(PMe_3)\}_2]^{2-}$, shown in Figure 9. The respective graph for a single $[SnB_{11}H_{11}]^{2-}$ unit is shown in the lower panel of Figure 8 (as above, this subunit was generated by removing from the system all atoms not belonging to the stannaborate unit, thus the electronic density plotted in the lower panel of Figure 8 refers to a point ~245 pm away from the Sn atom). We note in passing that one might have avoided the occurrence of positive orbital energies by employing the COSMO solvation model,[71] but as far as checked, this modification does not significantly change the sequence or shape of orbitals nor does it significantly change their density at the M−M bond. Again, the results for Ag and Au are qualitatively similar but quantitatively different. In both cases, the dominantly contributing orbital, 4, is identified as the nearly unchanged orbital m4 of the bare $[\{M(PMe_3)\}_2]^{2+}$ unit (here and in the following orbitals referring to the $[\{M(PMe_3)\}_2]^{2+}$ unit are labeled with prefix "m", those of the$[SnB_{11}H_{11}]^{2-}$ unit with "b", while those of the entire system have no prefix). Orbitals 1 and 2 are related to m1 and m2, but contributions from 1 and 2 to the M−M bond are smaller than for m1 and m2; they are mainly located at the PMe_3 ligands and not relevant for the M−M bond in $[\{M(PMe_3)(SnB_{11}H_{11})\}_2]^{2-}$. Instead, one observes contributions to the density in the cluster center from three further orbitals, 3, 5, and 6, that were not present in this form in the cationic subsystem. Orbitals 5 and 6 are symmetric/antisymmetric combinations of orbital m6 and the two b4 orbitals of the two $[SnB_{11}H_{11}]^{2-}$ units. Orbitals 5 and 6 are the energetically highest orbitals contributing to the M−M bond; nevertheless, they are ~1.5 eV below the HOMO, which mainly is a combination of the p_z orbital at Sn (*z* means parallel to the M−M axis) and

(71) Klamt, A.; Schürmann, G. *J. Chem. Soc., Perkin Trans.* **1993**, *2*, 799.

neighboring B atoms. Orbital 3 might be combined from the two b1 orbitals plus contributions from m3, m3′, and m5; contributions from the latter are more pronounced for Au than for Ag.

The electron density, resulting from these interactions, at the molecular center of the complete coordination compounds $[\{M(PMe_3)(SnB_{11}H_{11})\}_2]^{2-}$ is ~35% higher than the respective electron density in the bare cations $[\{M(PMe_3)\}_2]^{2+}$. Furthermore, also in the case of the entire anions, the electron density between the metal atoms and thus binding forces are significantly larger for Au than for Ag, leading to shorter M−M distances for Au than for Ag.

A similar procedure was applied to the tetramer, **6.** For the stannaborate-free system, $[\{Ag(PMe_3)\}_4]^{4+}$, the LUMO (Figure 10, upper part, left-hand side) is a totally symmetric combination of orbitals of the silver atoms with relatively high density at the molecular center. Optimization of the geometric structure (using the COSMO model[71] for compensation of positive charges thus preventing a Coulomb explosion) leads to a planar arrangement of the silver atoms. This changes when the LUMO is (even only partly) occupied: for $[\{Ag(PMe_3)\}_4]^{n+}$, $n = 3$, 2, the tetrahedral arrangement of Ag atoms is preferred, and this is also the effect of the stannaborate units. Like that for the dimer, combinations with the HOMOs of the stannaborate units stabilize the LUMO of $[\{Ag(PMe_3)\}_4]^{4+}$, allowing for occupation of this orbital (Figure 10, lower part, left-hand side) by electrons of the $[SnB_{11}H_{11}]^{2-}$ unit leading to the tetrahedral topology. Note that in the case of the dimer both orbitals 5 and 6 (Figure 9) are located at the M−M bond, as well as at the stannaborate units, whereas in the tetramer, the analogue of 6, shown in Figure 10, is located mainly at the M_4 tetrahedron and the analogue to orbital 5 (not shown in Figure 10) is mainly located at the stannaborate units.

The Ag triangle in the trimer, **5**, shows two longer bonds and one short bond. Again, the LUMO of the cationic subunit (Figure 10, upper part, right-hand side) is a symmetric combination of orbitals of the Ag atoms. The amplitude of this orbital is largest between the middle of the short axis and the center of the triangle (for an equilateral triangle it would be in the center of the triangle). As in the previous cases, for the entire system this orbital is stabilized by the HOMOs of the stannaborates (probably dominantly by the μ_2-bridging one) and filled with electrons from these orbitals (Figure 10, lower part, right-hand side). The present structure is preferred over a C_{3v}-symmetric structure with three μ_2-bridging stannaborate units not only because of steric reasons but also because the distance between the HOMOs of the $[SnB_{11}H_{11}]^{2-}$ units to the LUMO in the center of the cationic core is relatively large, thus hampering interactions.

We finally note that for **5** and **6** the electron density on the bond axes is higher by ~30% in the case of the analogous Au compounds (calculated for the same structure parameters). Furthermore, in the series dimer **4** to trimer **5** to tetramer **6**, the change of total electron density on the Ag−Ag axes after the addition of the stannaborate units decreases and the average Ag−Ag bond length increases in this sequence of compounds.

Summary and Conclusion

In this work, the first coordination compounds of the versatile stanna-*closo*-dodecaborate ligand with silver electrophiles are presented. The tin ligand readily forms bonds with silver and exhibits various bridging coordination modes at silver clusters. Depending on the size of the coordinating phosphine, we found a dimer with PPh_3, a trimer with PEt_3, and a tetramer with PMe_3. Without a coligand at the silver, a tetranuclear silver cluster surrounded by six borate ligands was characterized. The bonding situation and the role of the stannaborates can be most easily rationalized as an interaction of the LUMO of the cationic core (symmetric combination of dominantly Ag s-orbitals) with the HOMOs of the anionic $[SnB_{11}H_{11}]^{2-}$ units.

Acknowledgment. Dedicated to Professor Dieter Naumann on the occasion of his 65th birthday.

Supporting Information Available: Crystallographic data in CIF format for **4**, **5**, **6**, and **7**. This material is available free of charge via the Internet at http://pubs.acs.org.

IC700464D